https://doi.org/10.20965/jaciii.2020.p0738

Paper:

Noise Rejection Approaches for Various Rough Set-Based *C*-Means Clustering

Seiki Ubukata, Sho Sekiya, Akira Notsu, and Katsuhiro Honda

Osaka Prefecture University
1-1 Gakuen-cho, Nakaku, Sakai, Osaka 599-8531, Japan
E-mail: {subukata, notsu, honda}@cs.osakafu-u.ac.jp
[Received March 20, 2020; accepted August 21, 2020]

In the field of cluster analysis, rough set-based extensions of hard *C*-means (HCM; *k*-means) including rough *C*-means (RCM), rough set *C*-means (RSCM), and rough membership *C*-means (RMCM) are promising approaches for dealing with the certainty, possibility, uncertainty of belonging of object to clusters. Since *C*-means-type methods are strongly affected by noise, noise clustering approaches have been proposed. In noise clustering approaches, noise objects, which are far from any cluster center, are rejected for robust estimation. In this paper, we introduce noise rejection approaches for rough set-based *C*-means based on probabilistic memberships and propose noise RCM with membership normalization (NRCM-MN), noise RSCM with membership normalization (NRSCM-MN), and noise RMCM (NRMCM). In addition, visualization demonstration of the cluster boundaries on the two-dimensional plane of the proposed methods is carried out to confirm the characteristics of each method. Furthermore, the clustering performance is verified by numerical experiments using real-world datasets.

Keywords: rough set theory, noise clustering, rough *C*-means, rough set *C*-means, rough membership *C*-means

1. Introduction

Recently, huge amounts of data are accumulated and their effective utilization is required in society. In order to discover knowledge from large-scale data, the demand for the techniques for automatically classifying and summarizing the data is increasing. Clustering is one of the techniques for automatically classifying and summarizing data without supervision. A cluster is a group composed of objects that have similar features. The purpose of clustering is to extract an appropriate cluster structure from the data.

Hard *C*-means (HCM; *k*-means) [1] is one of the most widely used partitive clustering methods. However, HCM lacks flexibility because it assigns each object to one and only one cluster without considering the uncertainty inherent in the data. In order to overcome this problem, various approaches utilizing soft computing such as fuzzy theory [2] and rough set theory [3–5] have been proposed. Fuzzy *C*-means (FCM) [6, 7] was proposed as an extension of HCM based on fuzzy theory and is widely used as a flexible and robust method.

On the other hand, extensions of HCM based on rough set theory are attracting attention as promising approaches for dealing with the certainty, possibility, and uncertainty of belonging of object to clusters. Lingras and West first proposed rough *C*-means (LRCM) [8] and Peters proposed PRCM [9] with some refinements to LRCM. Ubukata et al. proposed generalized RCM (GRCM) [10] by integrating LRCM and PRCM. GRCM can express LRCM, PRCM, and their combination by tuning parameters. If no confusion arises, GRCM is simply called RCM. RCM allows each object to belong to multiple clusters by relaxing the condition of belonging based on a linear function of the distance to the nearest cluster. RCM is further generalized to linear function threshold-based *C*-means (LiFTCM) [11].

In principle, rough set theory deals with the certainty, possibility, and uncertainty by extracting the lower approximation, upper approximation, and boundary region, respectively. They are calculated by determining the belonging to any subset for each granule (neighborhood of object) in the space granulated by a binary relation. However, RCM-type methods do not correspond to the principle of rough set theory because the granulation of the object space is not considered. As a clustering model in granular space, Ubukata et al. proposed rough set *C*-means (RSCM) [12, 13].

In RCM and RSCM, aggregation strategies are required to determine the representative point (prototype) of the cluster, because each cluster is represented by three types of regions representing certainty, possibility, and uncertainty. In original methods, the priority weight of each region is set, and the aggregation is carried out by calculating the convex combination of the centers of three regions. If the distinction is necessary, we call these methods RCM with center combination (RCM-CC) and RSCM with center combination (RSCM-CC). These methods are difficult to use because we have to find and set the appropriate weight parameters. In order to overcome the problem, methods that determine the cluster center based on proba-

bilistic memberships are proposed. Peters proposed RCM with membership normalization (RCM-MN; πRCM) [14, 15] and Ubukata et al. proposed RSCM with membership normalization (RSCM-MN; πRSCM) [16]. These methods normalize the membership so that it satisfies the sum-to-one constraints across clusters. Ubukata et al. further proposed rough membership C-means (RMCM) [16, 17], which uses the rough membership (the proportion of cluster in the neighborhood of object) [18, 19] as a probabilistic membership.

In C-means-type methods, the cluster prototype is determined by the center, which is the point that minimizes the within-cluster sum of square errors. Therefore, C-means-type methods are strongly affected by outliers, which are objects with anomalous features. In noise clustering approaches, noise objects, which are far from any cluster center, are rejected for robust estimation. Dave proposed noise FCM (NFCM) [20, 21], in which a single noise cluster is introduced in addition to regular (non-noise) clusters and noise objects are rejected by assigning them to the noise cluster. Ubukata et al. proposed noise RCM-CC (NRCM-CC) and noise RSCM-CC (NRSCM-CC) as noise reduction approaches for RCM-CC and RSCM-CC [22]. NRCM-CC and NRSCM-CC realize flexible and robust clustering by considering the certainty, possibility, and uncertainty of belonging to the noise cluster as well as the regular clusters.

In rough clustering based on center combination, it is difficult to set the weight parameters. In noise rough clustering, it is more difficult because of an additional parameter, the noise distance. Therefore, in this study, we consider methods based on parameter-free center calculation, that is, methods based on the membership normalization or rough memberships. In this paper, noise rejection approaches for RCM, RSCM and RMCM are comprehensively discussed. In addition to our previously proposed NRCM-CC and NRSCM-CC, we introduce noise rejection approaches for rough set-based C-means based on probabilistic memberships and propose noise RCM-MN (NRCM-MN), noise RSCM-MN (NRSCM-MN), and noise RMCM (NRMCM). In addition, visualization demonstration of the cluster boundaries on the two-dimensional plane of the proposed methods is carried out to confirm the characteristics of each method. Furthermore, the clustering performance is verified by numerical experiments using real-world datasets.

The remainder of the paper is organized as follows. Section 2 describes the preliminaries for our study. Noise rejection approaches for various rough set-based C-means clustering are introduced and visualization demonstration is carried out in Section 3. In Section 4, our comparative experiments are discussed. Finally, the conclusions are presented in Section 5.

2. Preliminaries

In general, C-means-type clustering methods deal with a dataset composed of n objects with observations of m features. Let $U = \{\boldsymbol{x}_1, \ldots, \boldsymbol{x}_i, \ldots, \boldsymbol{x}_n\}$ be a set of objects, where each object is an m-dimensional real feature vector $\boldsymbol{x}_i = (x_{i1}, \ldots, x_{ij}, \ldots, x_{im})^\top$. Set the number of clusters, C, and extract C clusters composed of similar objects from U. The prototype of cluster c is represented by the cluster center $\boldsymbol{b}_c = (b_{c1}, \ldots, b_{cj}, \ldots, b_{cm})^\top$. Let $d_{ci} = ||\boldsymbol{x}_i - \boldsymbol{b}_c||$ be the Euclidean distance between $\boldsymbol{b}_c$ and $\boldsymbol{x}_i$. Let $D_{it} = ||\boldsymbol{x}_t - \boldsymbol{x}_i||$ be the Euclidean distance between $\boldsymbol{x}_i$ and $\boldsymbol{x}_t$.

2.1. Hard C-Means and Fuzzy C-Means

Let $u_{ci} \in \{0, 1\}$ be the membership value of object i to cluster c. If object i belongs to cluster c, then $u_{ci} = 1$, otherwise, $u_{ci} = 0$. HCM is formulated as follows to minimize the total within-cluster sum of squared errors.

$$\text{min.} \quad J_{HCM} = \sum_{c=1}^{C} \sum_{i=1}^{n} u_{ci} d_{ci}^2, \quad \ldots\ldots\ldots \quad (1)$$

$$s.t. \quad \sum_{c=1}^{C} u_{ci} = 1, \forall i, \quad \ldots\ldots\ldots \quad (2)$$

$$u_{ci} \in \{0, 1\}, \forall c, i. \quad \ldots\ldots\ldots \quad (3)$$

The update rules of u_{ci} and $\boldsymbol{b}_c$ are derived as follows, respectively:

$$u_{ci} = \begin{cases} 1 & \left(c = \underset{1 \le l \le C}{\arg\min}\, d_{li}\right), \\ 0 & (\text{otherwise}), \end{cases} \quad \ldots\ldots\ldots \quad (4)$$

$$\boldsymbol{b}_c = \frac{\sum_{i=1}^{n} u_{ci} \boldsymbol{x}_i}{\sum_{i=1}^{n} u_{ci}}. \quad \ldots\ldots\ldots \quad (5)$$

In HCM, the cluster centers are initialized, the memberships and centers are updated alternately until they converge.

In FCM, the membership value $u_{ci} \in [0, 1]$ is relaxed to take the value on the closed unit interval. The optimization problem is formulated as follows.

$$\text{min.} \quad J_{FCM} = \sum_{c=1}^{C} \sum_{i=1}^{n} u_{ci}^{\theta} d_{ci}^2, \quad \ldots\ldots\ldots \quad (6)$$

$$s.t. \quad \sum_{c=1}^{C} u_{ci} = 1, \forall i, \quad \ldots\ldots\ldots \quad (7)$$

$$u_{ci} \in [0, 1], \forall c, i, \quad \ldots\ldots\ldots \quad (8)$$

where θ ($\theta > 1$) is a parameter for adjusting the fuzziness degree. Larger θ produces a fuzzier partition. The update rules of u_{ci} and $\boldsymbol{b}_c$ are derived as follows, respectively:

$$u_{ci} = \frac{(d_{ci})^{\frac{2}{1-\theta}}}{\sum_{l=1}^{C}(d_{li})^{\frac{2}{1-\theta}}}, \quad \ldots\ldots\ldots\ldots\ldots (9)$$

$$\boldsymbol{b}_c = \frac{\sum_{i=1}^{n} u_{ci}^{\theta}\boldsymbol{x}_i}{\sum_{i=1}^{n} u_{ci}^{\theta}}. \quad \ldots\ldots\ldots\ldots\ldots (10)$$

In FCM, the membership values are initialized so that they satisfy the constraints, the centers and memberships are updated alternately until they converge.

2.2. Rough Set-Based *C*-Means

2.2.1. Rough *C*-Means

RCM considers the memberships of object to three regions with respect to cluster, namely, the lower area, upper area, and boundary area, in order to deal with the certainty, possibility, and uncertainty of belonging to clusters, respectively. Let $\underline{u}_{ci}, \overline{u}_{ci}, \hat{u}_{ci} \in \{0,1\}$ be the memberships of object i to the lower area, upper area, and boundary area of cluster c, respectively. In RCM object-cluster assignment, the membership to the upper area is first calculated. RCM allows each object to belong to multiple upper areas of clusters by relaxing the condition of belonging based on a linear function of the distance to the nearest cluster. The lower area is extracted as a region in which each object belongs to one and only one upper area of a cluster. The boundary area is extracted as a region in which each object belongs to multiple upper areas of clusters.

$\overline{u}_{ci}$, $\underline{u}_{ci}$, and $\hat{u}_{ci}$ are calculated as follows using the distance $d_i^{\min}$ to the nearest cluster:

$$d_i^{\min} = \min_{1\le l\le C} d_{li}, \quad \ldots\ldots\ldots\ldots\ldots (11)$$

$$\overline{u}_{ci} = \begin{cases} 1 & \left(d_{ci} \le \alpha d_i^{\min} + \beta\right), \\ 0 & (\text{otherwise}), \end{cases} \quad \ldots\ldots (12)$$

$$\underline{u}_{ci} = \begin{cases} 1 & \left(\overline{u}_{ci} = 1 \wedge \sum_{l=1}^{C} \overline{u}_{li} = 1\right), \\ 0 & (\text{otherwise}), \end{cases} \quad \ldots (13)$$

$$\hat{u}_{ci} = \begin{cases} 1 & \left(\overline{u}_{ci} = 1 \wedge \sum_{l=1}^{C} \overline{u}_{li} \ge 2\right), \\ 0 & (\text{otherwise}), \end{cases} \quad \ldots (14)$$

where α ($\alpha \ge 1$), β ($\beta \ge 0$) are parameters for adjusting the roughness. Larger α and β produce smaller lower areas, larger upper areas, and larger boundary areas.

Since each cluster is represented by three areas, aggregation strategies are required to calculate the cluster prototype. Here, we introduce two aggregation strategies.

One is RCM with center combination (RCM-CC), which is based on the convex combination of the centers of three areas.

$$\boldsymbol{b}_c = \begin{cases} \dfrac{\sum_{i=1}^{n} \overline{u}_{ci}\boldsymbol{x}_i}{\sum_{i=1}^{n} \overline{u}_{ci}} & \left(\sum_{i=1}^{n} \underline{u}_{ci} = 0 \vee \sum_{i=1}^{n} \hat{u}_{ci} = 0\right), \\ \underline{w}\dfrac{\sum_{i=1}^{n} \underline{u}_{ci}\boldsymbol{x}_i}{\sum_{i=1}^{n} \underline{u}_{ci}} + \overline{w}\dfrac{\sum_{i=1}^{n} \overline{u}_{ci}\boldsymbol{x}_i}{\sum_{i=1}^{n} \overline{u}_{ci}} + \hat{w}\dfrac{\sum_{i=1}^{n} \hat{u}_{ci}\boldsymbol{x}_i}{\sum_{i=1}^{n} \hat{u}_{ci}} & (\text{otherwise}), \end{cases} \quad (15)$$

where $\underline{w}, \overline{w}, \hat{w} \ge 0$ such that $\underline{w} + \overline{w} + \hat{w} = 1$ are weight parameters for three areas.

The other is RCM with membership normalization (RCM-MN), in which the cluster prototype is calculated by the normalized upper area membership $\tilde{u}_{ci}$ to satisfy the sum-to-one constraints across clusters.

$$\tilde{u}_{ci} = \frac{\overline{u}_{ci}}{\sum_{l=1}^{C} \overline{u}_{li}}, \quad \ldots\ldots\ldots\ldots\ldots (16)$$

$$\boldsymbol{b}_c = \frac{\sum_{i=1}^{n} \tilde{u}_{ci}\boldsymbol{x}_i}{\sum_{i=1}^{n} \tilde{u}_{ci}}. \quad \ldots\ldots\ldots\ldots\ldots (17)$$

This membership normalization strategy does not require setting of the weight parameters.

2.2.2. Rough Set *C*-Means

RSCM is a clustering model on a granulated object space. In RSCM, the object space U is previously granulated by a binary relation $\mathscr{R} \subseteq U \times U$. In this study, the binary relation is represented by the matrix-element form R_{it}. In the original method, R_{it} is determined as follows based on the neighborhood rough set model [23, 24]:

$$R_{it} = \begin{cases} 1 & (D_{it} \le \eta), \\ 0 & (\text{otherwise}), \end{cases} \quad \ldots\ldots\ldots (18)$$

$$\eta = \text{percentile}([D_{it}], \tau). \quad \ldots\ldots\ldots (19)$$

The neighborhood of object i is the set of objects within the distance η from i. It is useful to determine η by $\tau \in [0, 100]$ percentile of the distance distribution $[D_{it}]$. This allows setting the τ-percent of $[R_{it}]$ to be 1 independent of the scale of the feature space.

In each iteration of RSCM object-cluster assignment, temporary clusters are first generated by the HCM-based nearest-cluster assignment. The certainty, possibility, and uncertainty of belonging to clusters are represented by the lower approximation, upper approximation, and boundary region of temporary clusters with respect to $\mathscr{R}$. Let $\underline{u}_{ci}, \overline{u}_{ci}, \hat{u}_{ci} \in \{0,1\}$ be the memberships of the lower approximation, upper approximation, and boundary region, respectively. If no confusion arises, we use the same symbols as RCM.

Based on the definitions in the generalized rough set model [25], $\overline{u}_{ci}$, $\underline{u}_{ci}$, and $\hat{u}_{ci}$ are calculated as follows, respectively:

$$\overline{u}_{ci} = \begin{cases} 1 & \left(\dfrac{\sum_{t=1}^{n} R_{it} u_{ct}}{\sum_{t=1}^{n} R_{it}} > 0 \right), \\ 0 & (\text{otherwise}), \end{cases} \quad \ldots\ldots \quad (20)$$

$$\underline{u}_{ci} = \begin{cases} 1 & \left(\dfrac{\sum_{t=1}^{n} R_{it} u_{ct}}{\sum_{t=1}^{n} R_{it}} = 1 \right), \\ 0 & (\text{otherwise}), \end{cases} \quad \ldots\ldots \quad (21)$$

$$\hat{u}_{ci} = \begin{cases} 1 & \left(\dfrac{\sum_{t=1}^{n} R_{it} u_{ct}}{\sum_{t=1}^{n} R_{it}} \in (0,1) \right), \\ 0 & (\text{otherwise}). \end{cases} \quad \ldots\ldots \quad (22)$$

Two aggregation strategies for the calculation of the cluster prototypes are introduced in similar manner to RCM. One with Eq. (15) is called RSCM-CC. The other with Eqs. (16) and (17) is called RSCM-MN.

2.2.3. Rough Membership *C*-Means

In RMCM, the cluster center is calculated by the rough membership μ_{ci}, which is the proportion of cluster c in the neighborhood of object i.

$$\mu_{ci} = \frac{\sum_{t=1}^{n} R_{it} u_{ct}}{\sum_{t=1}^{n} R_{it}}, \quad \ldots\ldots\ldots\ldots \quad (23)$$

$$\boldsymbol{b}_c = \frac{\sum_{i=1}^{n} \mu_{ci} \boldsymbol{x}_i}{\sum_{i=1}^{n} \mu_{ci}} \quad \ldots\ldots\ldots\ldots \quad (24)$$

By using the rough membership, which is an intermediate product of rough approximation, more detailed neighborhood information can be utilized.

3. Noise Rejection Approaches for Various Rough Set-Based *C*-Means Clustering

In this paper, noise rejection approaches for RCM, RSCM and RMCM are comprehensively discussed. In addition to our previously proposed NRCM-CC and NRSCM-CC, we introduce noise rejection approaches for rough set-based *C*-means based on probabilistic memberships and propose noise RCM-MN (NRCM-MN), noise RSCM-MN (NRSCM-MN), and noise RMCM (NRMCM). In addition, visualization demonstration of the cluster boundaries on the two-dimensional plane of the proposed methods is carried out to confirm the characteristics of each method.

3.1. Noise Fuzzy *C*-Means

As a preliminary for the introduction of noise rough clustering, we explain one of the methods of noise fuzzy clustering. NFCM is one of the noise rejection approaches for FCM. In NFCM, a single noise cluster is introduced in addition to the regular clusters. Noise objects, which are far from any cluster center, are rejected by assigning them to the noise cluster for robust estimation. Let C be the number of clusters including $C-1$ regular clusters and one noise cluster. Let C-th cluster be the noise cluster.

The optimization problem of NFCM is formulated as follows:

$$\text{min. } J_{NFCM} = \sum_{c=1}^{C-1} \sum_{i=1}^{n} u_{ci}^{\theta} d_{ci}^2 + \delta^2 \sum_{i=1}^{n} u_{Ci}^{\theta},$$

under the same constraints as FCM, where δ ($\delta \geq 0$) is the noise distance, which is the reference value for noise determination. Smaller δ rejects more objects as noise. NFCM can be implemented in a simple manner by fixing the distance $d_{Ci} = \delta$, which is the distance between object i and the noise cluster, in FCM.

3.2. Algorithms of Proposed Methods

This subsection shows the algorithms of the proposed methods. The noise rejection schemes of the proposed methods are implemented by similar manners to the derivation of NFCM from FCM. That is, in each iteration, the memberships are calculated by fixing $d_{Ci} = \delta$ and the prototypes of the regular clusters ($1 \leq c \leq C-1$) are calculated.

The conventional methods and the proposed methods are summarized in **Table 1**.

3.2.1. Noise RCM

A sample algorithm of NRCM including NRCM-CC and NRCM-MN is shown in **Algorithm 1**. Note that, membership normalization is executed including the noise cluster as well as the regular clusters.

3.2.2. Noise RSCM

A sample algorithm of NRSCM including NRSCM-CC and NRSCM-MN is shown in **Algorithm 2**. Note that, membership normalization is executed including the noise cluster as well as the regular clusters.

3.2.3. Noise RMCM

A sample algorithm of NRMCM is shown in **Algorithm 3**.

Table 1. Summary of the conventional methods and the proposed methods. The methods with '*' are the proposed methods.

Summary	Center Calculation	RCM-type	RSCM-type	RMCM-type
Without Noise Rejection	Center Combination	RCM-CC	RSCM-CC	RMCM
	Membership Normalization	RCM-MN	RSCM-MN	
Noise Rejection	Center Combination	NRCM-CC	NRSCM-CC	NRMCM *
	Membership Normalization	NRCM-MN *	NRSCM-MN *	

Algorithm 1 NRCM

Step 1. Set C ($1 < C < n$), α ($\alpha \geq 1$), β ($\beta \geq 0$), and δ ($\delta \geq 0$).
Step 2. Initialize $\boldsymbol{b}_c$.
Step 3. Calculate $\overline{u}_{ci}$, $\underline{u}_{ci}$, and $\hat{u}_{ci}$ using Eqs. (11), (12), (13), and (14), fixing $d_{Ci} = \delta$.
Step 4. Calculate $\boldsymbol{b}_c$ ($1 \leq c \leq C-1$):
if NRCM-CC **then**
  Using Eq. (15) with $\underline{w}, \overline{w}, \hat{w} \geq 0$
  such that $\underline{w} + \overline{w} + \hat{w} = 1$.
else if NRCM-MN **then**
  Using Eqs. (16) and (17).
end if
Step 5. Repeat **Steps 3–4** until $\overline{u}_{ci}$ do not change.

Algorithm 2 NRSCM

Step 1. Set C ($1 < C < n$), $[R_{it}]$, and δ ($\delta \geq 0$).
Step 2. Initialize $\boldsymbol{b}_c$.
Step 3. Calculate u_{ci}, $\overline{u}_{ci}$, $\underline{u}_{ci}$, and $\hat{u}_{ci}$ using Eqs. (4), (20), (21), and (22), fixing $d_{Ci} = \delta$.
Step 4. Calculate $\boldsymbol{b}_c$ ($1 \leq c \leq C-1$):
if NRSCM-CC **then**
  Using Eq. (15) with $\underline{w}, \overline{w}, \hat{w} \geq 0$
  such that $\underline{w} + \overline{w} + \hat{w} = 1$.
else if NRSCM-MN **then**
  Using Eqs. (16) and (17).
end if
Step 5. Repeat **Steps 3–4** until u_{ci} do not change.

Algorithm 3 NRMCM

Step 1. Set C ($1 < C < n$), $[R_{it}]$, and δ ($\delta \geq 0$).
Step 2. Initialize $\boldsymbol{b}_c$.
Step 3. Calculate u_{ci} and μ_{ci} using Eqs. (4) and (23), fixing $d_{Ci} = \delta$.
Step 4. Calculate $\boldsymbol{b}_c$ ($1 \leq c \leq C-1$) using Eq. (24).
Step 5. Repeat **Steps 3–4** until u_{ci} do not change.

3.3. Cluster Boundary Visualization

This subsection shows the visualization demonstration of the cluster boundaries on the two-dimensional plane of the proposed methods. We generated an artificial dataset, grid data, in which $n = 100 \times 100$ objects are equally arranged in a grid on the unit square $[0,1] \times [0,1]$. We consider extracting three regular clusters, $c = (1,2,3)$, and one noise cluster, $c = 4$, in the grid data. That is, we show the results of the proposed methods with the cluster number $C = 4$. The regular clusters, $c = (1,2,3)$, correspond to the primary colors $(red, green, blue)$, respectively. The noise cluster, $c = 4$, corresponds to black.

In NRCM and NRSCM, the RGB value $(r,g,b)_i$ of object i is calculated as follows based on resulting $\overline{u}_{ci}$:

$$(r,g,b)_i = \begin{cases} 255 \times (\overline{u}_{1i}, \overline{u}_{2i}, \overline{u}_{3i}) & \\ & (\overline{u}_{4i} = 0), \\ 255 \times \left(\dfrac{\overline{u}_{1i}}{\sum_{c=1}^{C} \overline{u}_{ci}}, \dfrac{\overline{u}_{2i}}{\sum_{c=1}^{C} \overline{u}_{ci}}, \dfrac{\overline{u}_{3i}}{\sum_{c=1}^{C} \overline{u}_{ci}} \right) & \\ & (\overline{u}_{4i} = 1). \end{cases}$$

Objects belonging to one and only one regular cluster are displayed in primary colors. Objects belonging to the boundary area (region) of multiple regular clusters are displayed in additive color mixture. Objects belonging to the boundary area (region) of the noise cluster are darkened by dividing the membership. Objects only belonging to the noise cluster are displayed in black.

In NRMCM, the RGB value $(r,g,b)_i$ of the object i is calculated as follows based on resulting μ_{ci}:

$$(r,g,b)_i = 255 \times (\mu_{1i}, \mu_{2i}, \mu_{3i}).$$

The RGB values are distributed based on the proportion of clusters in the neighborhood of object. Objects closer to primary colors have higher certainty of belonging to a regular cluster.

In order to observe the cluster boundaries under the same condition, the centers of the three regular clusters, $c = (1,2,3)$, are fixed as follows, respectively:

$$\boldsymbol{b}_1 = (0.22, 0.31)^\top,$$
$$\boldsymbol{b}_2 = (0.5, 0.81)^\top,$$
$$\boldsymbol{b}_3 = (0.78, 0.31)^\top.$$

These cluster centers are one of the results of HCM. Each center of the regular cluster is indicated by the cross mark in the figures. The noise cluster does not have the center. Since the centers are fixed, differences in the center calculation methods (CC and MN) are not considered in this demonstration.

Figure 1 shows the result of NRCM ($\alpha = 1$, $\beta = 0$), in which a hard partition is obtained and no boundary area

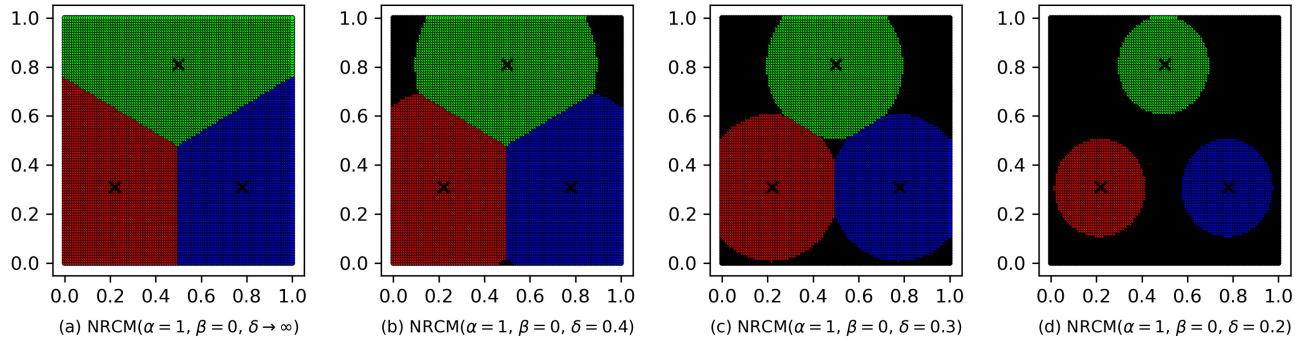

Fig. 1. Grid data: Visualization of the cluster boundaries by NRCM ($\alpha = 1$, $\beta = 0$) for each $\delta \in \{\infty, 0.4, 0.3, 0.2\}$.

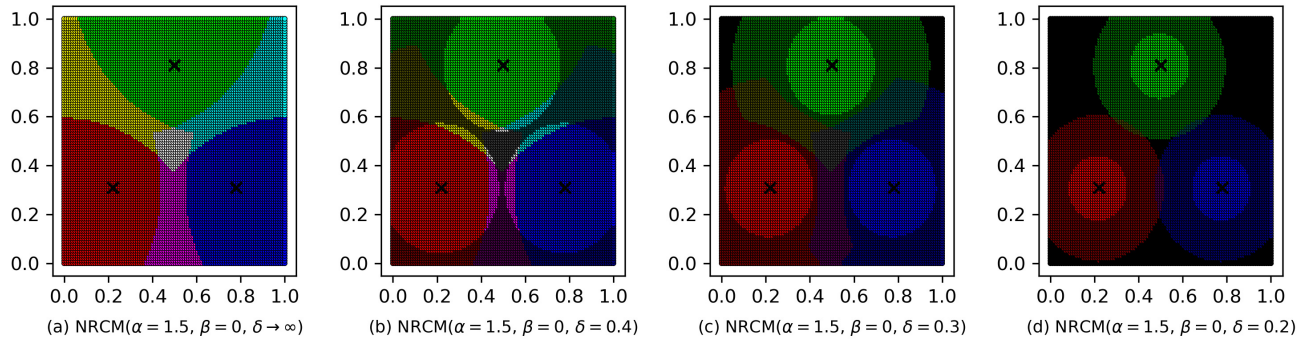

Fig. 2. Grid data: Visualization of the cluster boundaries by NRCM ($\alpha = 1.5$, $\beta = 0$) for each $\delta \in \{\infty, 0.4, 0.3, 0.2\}$.

is detected. **Fig. 1(a)** shows the result of $\delta \to \infty$, in which noise objects are not detected. This is the same result as HCM, which produces the Voronoi boundary. **Fig. 1(b)** shows the result of $\delta = 0.4$. By reducing δ, black regions appear at the top both ends. That is, objects far from any cluster center are rejected as noise. **Fig. 1(c)** shows the result of $\delta = 0.3$. By further reducing δ, black areas are enlarged rejecting more objects as noise. **Fig. 1(d)** shows the result of $\delta = 0.2$. By further reducing δ, circular regular clusters are finally extracted.

Figure 2 shows the results of NRCM ($\alpha = 1.5$, $\beta = 0$). **Fig. 2(a)** shows the result of $\delta \to \infty$, in which noise objects are not detected. By increasing α, the boundary areas are detected assigning objects to multiple clusters. Since the boundary area is calculated based on the distance ratio, it forms the circles of Apollonius. **Fig. 2(b)** shows the result of $\delta = 0.4$. By reducing δ, dark areas, in which objects possibly belong to the noise cluster, appear. **Fig. 2(c)** shows the result of $\delta = 0.3$. By further reducing δ, black areas, in which objects certainly belong to the noise cluster, appear. **Fig. 2(d)** shows the result of $\delta = 0.2$. By further reducing δ, double circular regular clusters, in which the upper area includes the lower area, are finally extracted.

Figure 3 shows the results of NRCM ($\alpha = 1$, $\beta = 0.15$). **Figs. 3(a)**, **(b)**, **(c)**, and **(d)** show similar trends to **Figs. 2(a)**, **(b)**, **(c)**, and **(d)**, respectively. Since the boundary area is calculated based on the distance difference, it forms hyperbolas. The ratio of the lower area and upper area is different from **Fig. 2**, because it is different whether the distance ratio is used or the distance difference is used.

Figure 4 shows the results of NRSCM ($\tau = 3$). **Figs. 4(a)**, **(b)**, **(c)**, and **(d)** correspond to the results of the upper approximation of the hard partitions in **Figs. 1(a)**, **(b)**, **(c)**, and **(d)**, respectively, and show similar trends to **Figs. 2** and **3**. Since the boundary region is calculated based on neighborhood information, it forms more complex shape than that of NRCM. The roundness and sharpness of the boundary regions in **Fig. 4** are attributed to the sharp parts of the noise cluster in **Fig. 1**.

Figure 5 shows the results of NRMCM ($\tau = 3$). Since the rough membership is an intermediate product of the upper approximation, the rough memberships in **Figs. 5(a)**, **(b)**, **(c)**, and **(d)** induce the upper approximations in **Figs. 4(a)**, **(b)**, **(c)**, and **(d)** by threshold processing, respectively. Since the rough membership takes a real value, the clusters are expressed by gradation. **Fig. 5(a)** shows the result of $\delta \to \infty$, in which noise objects are not detected. Here, objects in dark areas have the uncertainty of belonging to the regular clusters. When δ is decreased in the order of **Figs. 5(b)**, **(c)**, and **(d)**, the dark area surrounding the regular clusters expands. Here, dark areas have the uncertainty of belonging to the noise clusters as well as the regular clusters.

It was shown that NRCM, NRSCM, and NRMCM pro-

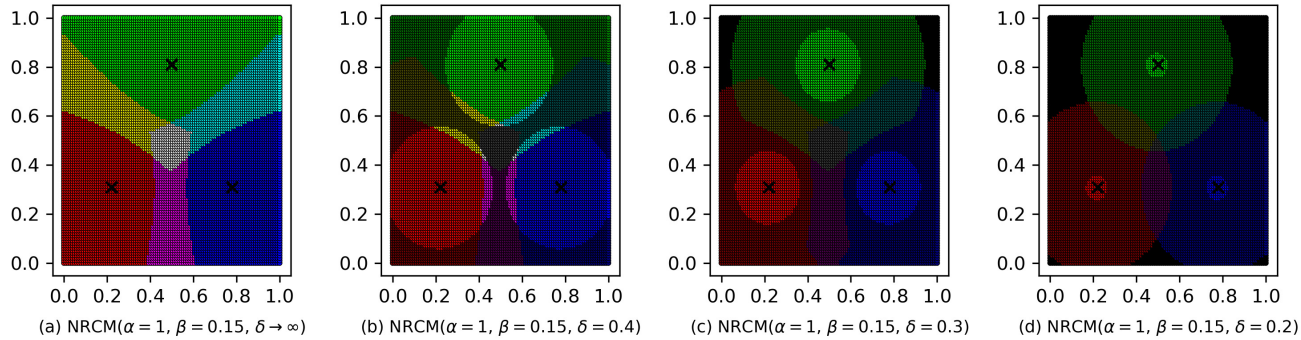

Fig. 3. Grid data: Visualization of the cluster boundaries by NRCM ($\alpha = 1$, $\beta = 0.15$) for each $\delta \in \{\infty, 0.4, 0.3, 0.2\}$.

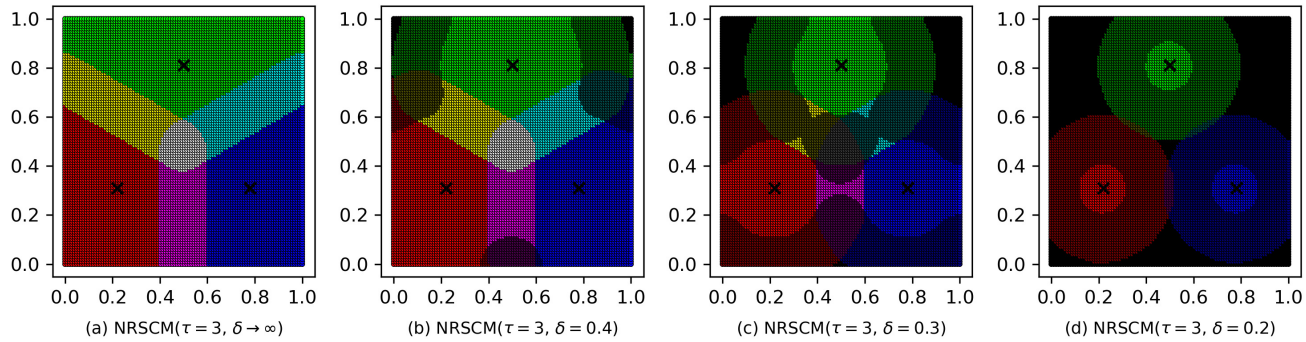

Fig. 4. Grid data: Visualization of the cluster boundaries by NRSCM ($\tau = 3$) for each $\delta \in \{\infty, 0.4, 0.3, 0.2\}$.

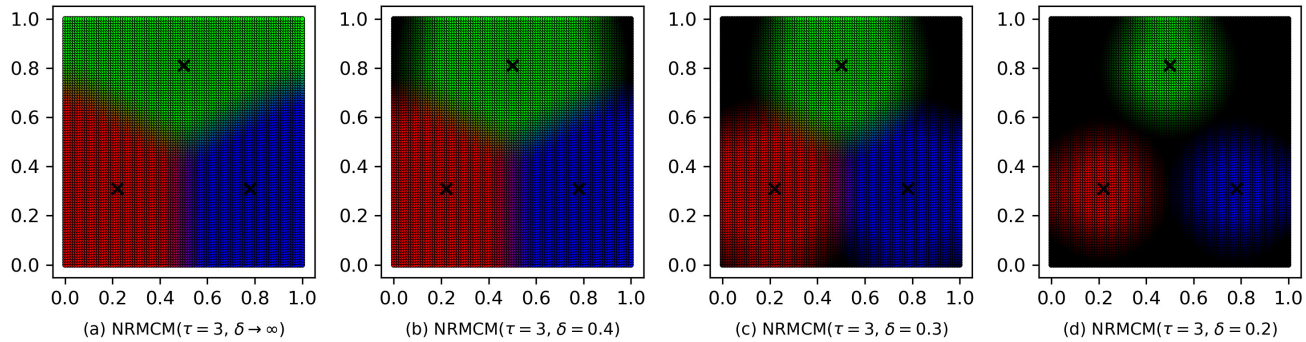

Fig. 5. Grid data: Visualization of the cluster boundaries by NRMCM ($\tau = 3$) for each $\delta \in \{\infty, 0.4, 0.3, 0.2\}$.

duce the cluster boundaries with different characteristics considering the certainty, possibility, uncertainty of belonging to the noise cluster as well as the regular clusters.

4. Numerical Experiments

In this section, we verify the clustering performance of the proposed methods using real-world datasets by evaluating the estimation performance of the true class centers. In datasets, each object has the true class label as well as the observations of the features. Let $\boldsymbol{b}_l^{\text{true}}$ be the true center of class l. By setting the number of clusters C as the number of classes plus one (the one is for the noise cluster), clustering was performed to obtain the regular cluster center $\boldsymbol{b}_c$ ($1 \leq c \leq C-1$) without supervision, that is, without class information.

The center error (CE), which is the sum of errors between the resulting regular cluster centers and corresponding true class centers, was calculated as follows:

$$CE = \sum_{c=1}^{C-1} ||\boldsymbol{b}_c - \boldsymbol{b}_c^{\text{true}}||, \quad \ldots\ldots\ldots \quad (25)$$

where the one-to-one correspondence between the regular clusters and classes was selected so that it minimizes CE. The smaller the CE is, the more accurately the class struc-

ture can be estimated without supervision. Since it is difficult to compare the consistency between the given label structure, which has no overlap and no noise, and the resulting cluster structure, which has overlap and noise, we evaluate the performance by *CE*, which is easy to compare. We assume that if latent overlap and noise are handled properly then the cluster center can be estimated more accurately.

To avoid the initial value dependence of clustering, the initial cluster centers was determined by the result of HCM with the strict KKZ initialization, in which the first two centers are set by the most distant two objects and the subsequent centers are set by the most distant object from the nearest center.

4.1. Iris Dataset

This subsection shows the results for the Iris dataset downloaded from the UCI Machine Learning Repository [26]. The Iris dataset consists of $n = 150$ objects, $m = 4$ features ($\{sepal\_length, sepal\_width, petal\_length, petal\_width\}$), and three classes ($\{setosa, versicolour, virginica\}$).

Figure 6 shows the result of NRCM ($\alpha = 1$, $\beta = 0$) changing $\delta \in [0.3, 2.5]$ in increments of 0.01. Since this is the case of hard noise clustering, NRCM-CC and NRCM-MN produce the same result. In the case of $\delta \geq 1.7$, no object is detected as noise and the result is the same as that of HCM. In the case of $\delta \in [0.5, 1.5]$, a certain number of objects is rejected as noise, improving the performance. In the case of $\delta < 0.5$, more objects are rejected as noise and the regular clusters shrink, degrading the performance.

We compared the performances of two center calculation methods, namely, the center combination and the membership normalization, under the condition, $\delta \to \infty$, in which noise rejection was not performed. **Fig. 7** shows the results of NRCM-CC ($\delta \to \infty$, $\beta = 0$) changing $\alpha \in [1, 3]$ in increments of 0.05 for various weights, where $w = (\underline{w}, \overline{w}, \hat{w})$, and NRCM-MN ($\delta \to \infty$, $\beta = 0$). **Fig. 8** shows the results of NRCM-CC ($\delta \to \infty$, $\alpha = 1$) changing $\beta \in [0, 1.5]$ in increments of 0.05 for various weights and NRCM-MN ($\delta \to \infty$, $\alpha = 1$). In both cases, the performance deteriorates when the weight $\hat{w}$ of the boundary area is given. Although $w = (1.0, 0.0, 0.0)$ and $w = (0.5, 0.5, 0.0)$ produce better performance, it is difficult to set an appropriate combination of the weight parameters. NRCM-MN can produce relatively stable performance without weight setting. Thereafter, we use the membership normalization-based methods to compare NRCM, NRSCM, and NRMCM.

Figure 9 shows the results of NRCM-MN ($\beta = 0$) changing $\alpha \in [1, 3]$ in increments of 0.05 for each $\delta \in \{\infty, 1.5, 1.25, 1.0, 0.75, 0.5\}$. **Fig. 10** shows the results of NRCM-MN ($\alpha = 1$) changing $\beta \in [0, 1.5]$ in increments of 0.05 for each $\delta \in \{\infty, 1.5, 1.25, 1.0, 0.75, 0.5\}$. For all δ, the performance is improved by increasing α or β to some extent, whereas it is degraded by further increasing the parameters. That is, the appropriate roughness improves the performance. $\delta \to \infty$ is the result of not rejecting noise. The appropriate adjustment of δ improves the performance. In this case, the best result is $CE = 0.213$

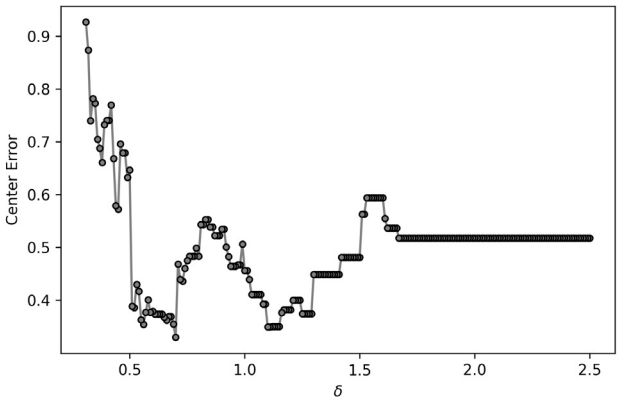

Fig. 6. Iris: Transition of center error by NRCM ($\alpha = 1$, $\beta = 0$) changing $\delta \in [0.3, 2.5]$ in increments of 0.01.

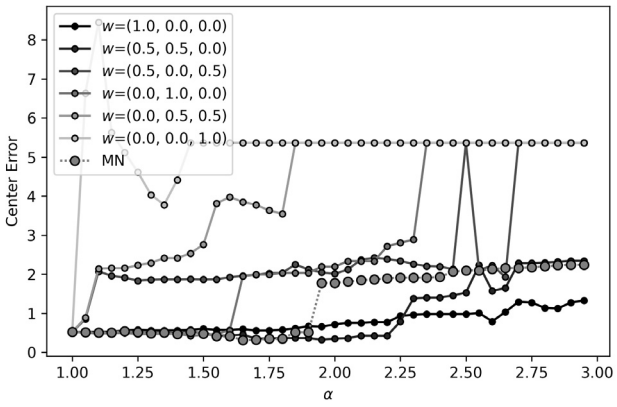

Fig. 7. Iris: Transition of the center error by NRCM-CC ($\delta \to \infty$, $\beta = 0$) changing $\alpha \in [1, 3]$ in increments of 0.05 for various weights and NRCM-MN ($\delta \to \infty$, $\beta = 0$).

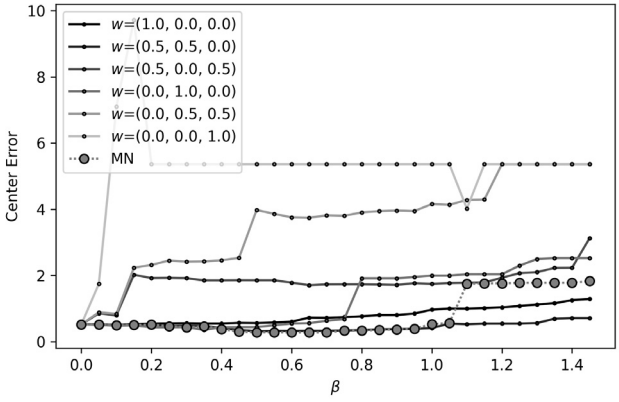

Fig. 8. Iris: Transition of the center error by NRCM-CC ($\delta \to \infty$, $\alpha = 1$) changing $\beta \in [0, 1.5]$ in increments of 0.05 for various weights and NRCM-MN ($\delta \to \infty$, $\alpha = 1$).

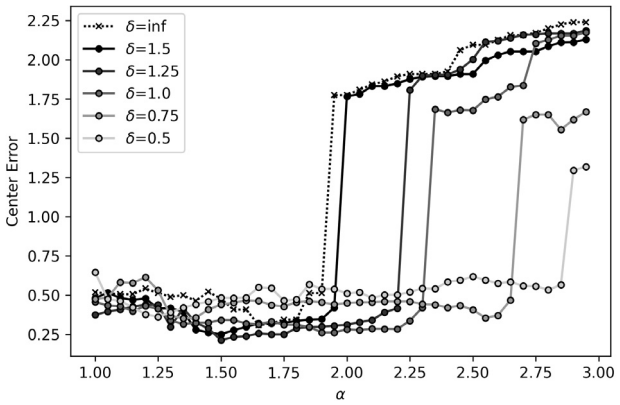

Fig. 9. Iris: Transitions of the center error by NRCM-MN ($\beta = 0$) changing $\alpha \in [1,3]$ in increments of 0.05 for each $\delta \in \{\infty, 1.5, 1.25, 1.0, 0.75, 0.5\}$.

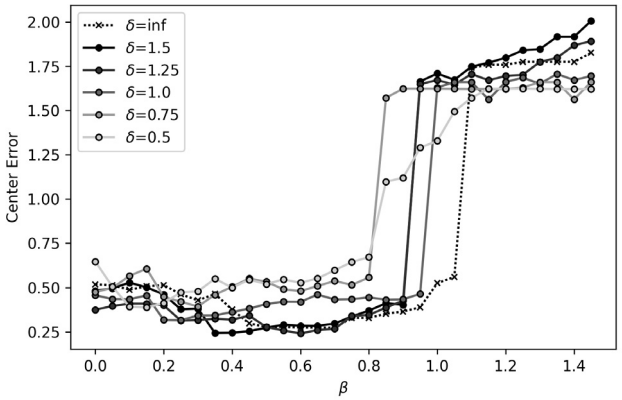

Fig. 10. Iris: Transitions of the center error by NRCM-MN ($\alpha = 1$) changing $\beta \in [0,1.5]$ in increments of 0.05 for each $\delta \in \{\infty, 1.5, 1.25, 1.0, 0.75, 0.5\}$.

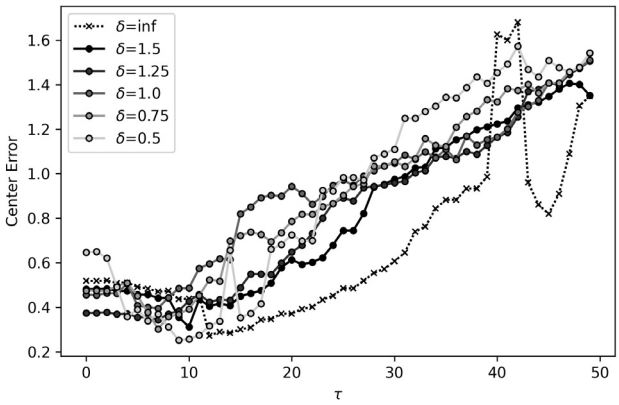

Fig. 11. Iris: Transitions of the center error by NRSCM-MN changing $\tau \in [0,50]$ in increments of 1 for each $\delta \in \{\infty, 1.5, 1.25, 1.0, 0.75, 0.5\}$.

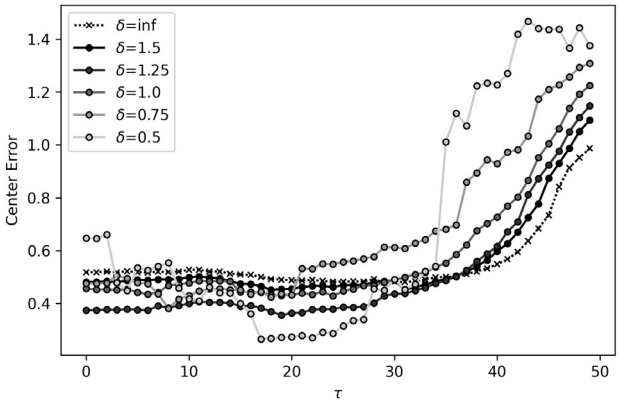

Fig. 12. Iris: Transitions of the center error by NRMCM changing $\tau \in [0,50]$ in increments of 1 for each $\delta \in \{\infty, 1.5, 1.25, 1.0, 0.75, 0.5\}$.

when $\alpha = 1.5$ and $\delta = 1.25$. **Fig. 11** shows the results of NRSCM-MN changing $\tau \in [0,50]$ in increments of 1 for each $\delta \in \{\infty, 1.5, 1.25, 1.0, 0.75, 0.5\}$. In this case, the best result is $CE = 0.256$ when $\tau = 9$ and $\delta = 0.5$. **Fig. 12** shows the results of NRMCM changing $\tau \in [0,50]$ in increments of 1 for each $\delta \in \{\infty, 1.5, 1.25, 1.0, 0.75, 0.5\}$. In this case, the best result is $CE = 0.265$ when $\tau = 17$ and $\delta = 0.5$. Therefore, the appropriate roughness and noise rejection improves the performance.

4.2. Breast Cancer Wisconsin Dataset

This subsection shows the results for the Breast Cancer Wisconsin (BCW) dataset downloaded from the UCI Machine Learning Repository [26]. The BCW dataset consists of $n = 569$ objects, $m = 30$ features, and two classes ($\{malignant, benign\}$).

Figures 13, **14**, **15**, **16**, **17**, **18**, and **19** show the results of similar settings to **Figs. 6**, **7**, **8**, **9**, **10**, **11**, and **12**, respectively, changing $\alpha \in [1,1.8]$ in increments of 0.05, $\beta \in [0,3]$ in increments of 0.1 for each $\delta \in \{\infty, 15, 12.5, 10, 7.5, 5\}$. They show similar trends to the Iris dataset.

NRCM-MN ($\alpha = 1$, $\beta = 0$) produced the best result $CE = 0.773$ when $\delta = 7.5$. Similar to the Iris dataset, the membership normalization can produce relatively stable performance without weight setting. NRCM-MN ($\beta = 0$) produced the best result $CE = 0.708$ when $\alpha = 1.2$ and $\delta = 7.5$. NRCM-MN ($\alpha = 1$) produced the best result $CE = 0.712$ when $\beta = 1.2$ and $\delta = 7.5$. NRSCM-MN produced the best result $CE = 0.755$ when $\tau = 2$ and $\delta = 7.5$. NRMCM-MN produced the best result $CE = 0.743$ when $\tau = 18$ and $\delta = 7.5$.

From the above experimental results, it was shown that the estimation performance of the true class centers was improved by the proposed methods with appropriate roughness and noise rejection.

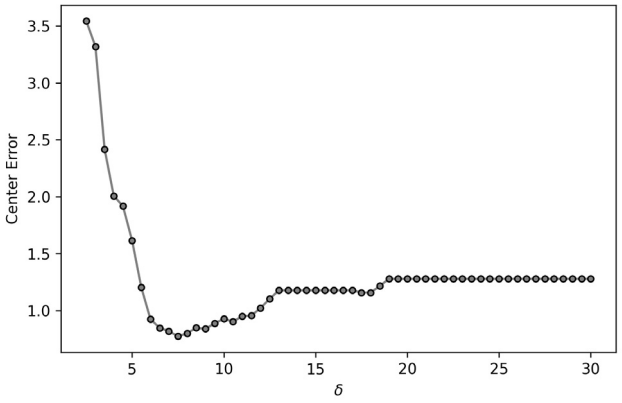

Fig. 13. BCW: Transition of the center error by NRCM-MN ($\alpha = 1, \beta = 0$) changing $\delta \in [0.3, 2.5]$ in increments of 0.01.

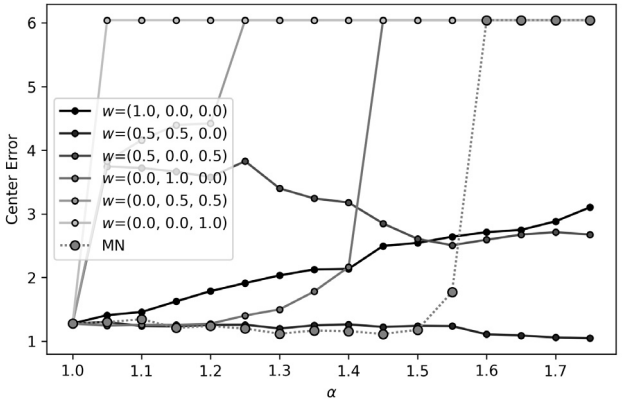

Fig. 14. BCW: Transition of the center error by NRCM-CC ($\delta \to \infty, \beta = 0$) changing $\alpha \in [1, 1.8]$ in increments of 0.05 for various weights and NRCM-MN ($\delta \to \infty, \beta = 0$).

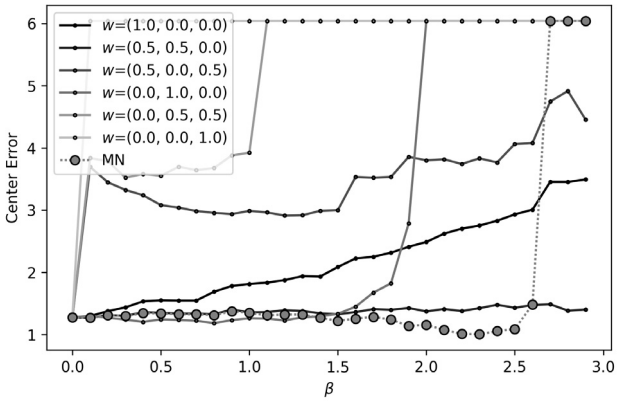

Fig. 15. BCW: Transition of the center error by NRCM-CC ($\delta \to \infty, \alpha = 1$) changing $\beta \in [0, 3]$ in increments of 0.1 for various weights and NRCM-MN ($\delta \to \infty, \alpha = 1$).

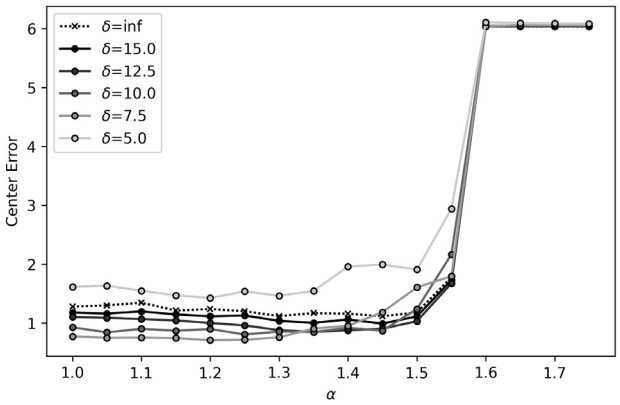

Fig. 16. BCW: Transitions of the center error by NRCM-MN ($\beta = 0$) changing $\alpha \in [1, 1.8]$ in increments of 0.05 for each $\delta \in \{\infty, 15, 12.5, 10, 7.5, 5\}$.

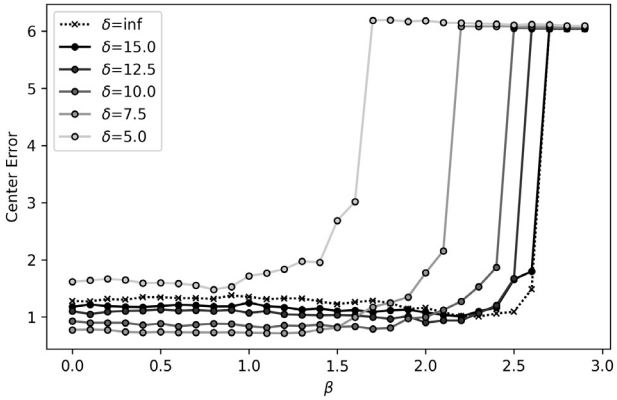

Fig. 17. BCW: Transitions of the center error by NRCM-MN ($\alpha = 1$) changing $\beta \in [0, 3]$ in increments of 0.1 for each $\delta \in \{\infty, 15, 12.5, 10, 7.5, 5\}$.

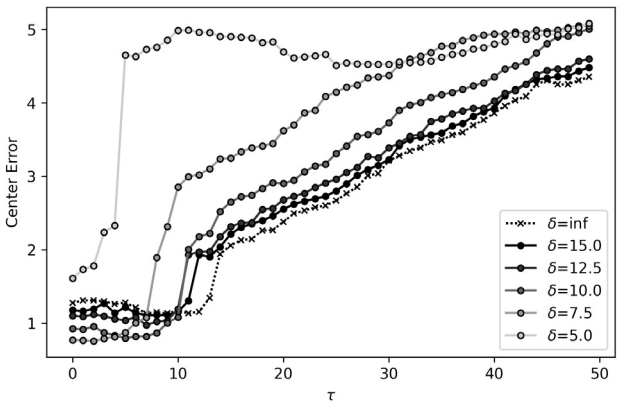

Fig. 18. BCW: Transitions of the center error by NRSCM-MN changing $\tau \in [0, 50]$ in increments of 1 for each $\delta \in \{\infty, 15, 12.5, 10, 7.5, 5\}$.

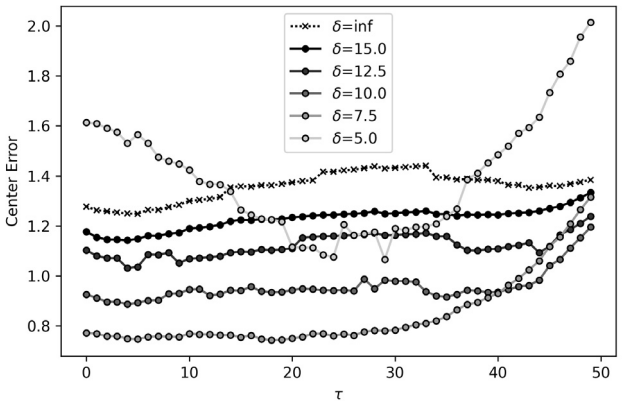

Fig. 19. BCW: Transitions of the center error by NRMCM changing $\tau \in [0,50]$ in increments of 1 for each $\delta \in \{\infty, 15, 12.5, 10, 7.5, 5\}$.

5. Conclusions

In this paper, noise rejection approaches for RCM, RSCM and RMCM were comprehensively discussed. In addition to our previously proposed NRCM-CC and NRSCM-CC, we introduced noise rejection approaches for rough set-based *C*-means based on probabilistic memberships and proposed NRCM-MN, NRSCM-MN, and NRMCM. In addition, visualization demonstration of the cluster boundaries on the two-dimensional plane of the proposed methods was carried out to confirm the characteristics of each method. It was shown that NRCM, NRSCM, and NRMCM produce the cluster boundaries with different characteristics considering the certainty, possibility, uncertainty of belonging to the noise cluster as well as the regular clusters. Furthermore, the clustering performance was verified by numerical experiments using real-world datasets. It was shown that the estimation performance of the true class centers was improved by the proposed methods with appropriate roughness and noise rejection. The appropriate roughness and noise distance were indicated in the two datasets, namely, the Iris dataset and the Breast Cancer Wisconsin dataset. However, it is difficult to know the appropriate roughness and noise distance in advance in actual data analysis tasks, and empirical tuning is required. Therefore, the adjustment of appropriate parameters is a future task. On the other hand, the proposed methods based on the membership normalization or rough memberships are expected to achieve stable performance without weight setting in the center combination.

We plan to consider automatic determination of the parameters with respect to the roughness and noise rejection.

Acknowledgements

This work was partly supported by JSPS KAKENHI Grant Numbers JP17K12753, and Program to Disseminate Tenure Tracking System, MEXT, Japan.

References:

[1] J. MacQueen, "Some Methods for Classification and Analysis of Multivariate Observations," Proc. of the 5th Berkeley Symp. on Mathematical Statistics and Probability, pp. 281-297, 1967.
[2] L. A. Zadeh, "Fuzzy sets," Information and Control, Vol.8, Issue 3, pp. 338-353, 1965.
[3] Z. Pawlak, "Rough sets," Int. J. of Computer & Information Sciences, Vol.11, Issue 5, pp. 341-356, 1982.
[4] Z. Pawlak, "Rough classification," Int. J. of Man-Machine Studies, Vol.20, Issue 5, pp. 469-483, 1984.
[5] Z. Pawlak, "Rough set approach to knowledge-based decision support," European J. of Operational Research, Vol.99, Issue 1, pp. 48-57, 1997.
[6] J. C. Bezdek, "Pattern Recognition with Fuzzy Objective Function Algorithms," Plenum Press, 1981.
[7] J. C. Dunn, "A Fuzzy Relative of the ISODATA Process and Its Use in Detecting Compact Well-Separated Clusters," J. of Cybernetics, Vol.3, Issue 3, pp. 32-57, 1973.
[8] P. Lingras and C. West, "Interval Set Clustering of Web Users with Rough *K*-Means," J. of Intelligent Information Systems, Vol.23, Issue 1, pp. 5-16, 2004.
[9] G. Peters, "Some refinements of rough *k*-means clustering," Pattern Recognition, Vol.39, Issue 8, pp. 1481-1491, 2006.
[10] S. Ubukata, A. Notsu, and K. Honda, "General Formulation of Rough C-Means Clustering," Int. J. of Computer Science and Network Security, Vol.17, No.9, pp. 29-38, 2017.
[11] S. Ubukata, "A Unified Approach for Cluster-Wise and General Noise Rejection Approaches for K-Means Clustering," PeerJ Computer Science, 5:e238, doi: 10.7717/peerj-cs.238, 2019.
[12] S. Ubukata, A. Notsu, and K. Honda, "The Rough Set k-Means Clustering," Proc. of 2016 Joint 8th Int. Conf. on Soft Computing and Intelligent Systems (SCIS) and 17th Int. Symp. on Advanced Intelligent Systems (ISIS), pp. 189-193, 2016.
[13] S. Ubukata, A. Notsu, and K. Honda, "Characteristics of Rough Set *C*-Means Clustering," J. Adv. Comput. Intell. Intell. Inform., Vol.22, No.4, pp. 551-564, 2018.
[14] G. Peters, "Rough clustering utilizing the principle of indifference," Information Sciences, Vol.277, pp. 358-374, 2014.
[15] G. Peters, "Is there any need for rough clustering?," Pattern Recognition Letters, Vol.53, pp. 31-37, 2015.
[16] S. Ubukata, H. Kato, A. Notsu, and K. Honda, "Rough Set-Based Clustering Utilizing Probabilistic Memberships," J. Adv. Comput. Intell. Intell. Inform., Vol.22, No.6, pp. 956-964, 2018.
[17] S. Ubukata, A. Notsu, and K. Honda, "The Rough Membership *k*-Means Clustering," Proc. of the 5th Int. Symp. on Integrated Uncertainty in Knowledge Modelling and Decision Making (IUKM 2016), pp. 207-216, 2016.
[18] Z. Pawlak and A. Skowron, "Rough membership functions: a tool for reasoning with uncertainty," C. Rauszer (Ed.), "Algebraic Methods in Logic and Computer Science," Banach Center Publications, Vol.28, pp. 135-150, Institute of Mathematics, Polish Academy of Science, 1993.
[19] Z. Pawlak and A. Skowron, "Rough membership functions," R. R. Yager, J. Kacprzyk, and M. Fedrizzi (Eds.), "Advances in the Dempster-Shafer Theory of Evidence," pp. 251-271, John Wiley & Sons, Inc., 1994.
[20] R. N. Dave, "Characterization and detection of noise in clustering," Pattern Recognition Letters, Vol.12, No.11, pp. 657-664, 1991.
[21] R. N. Dave and R. Krishnapuram, "Robust clustering methods: a unified view," IEEE Trans. on Fuzzy Systems, Vol.5, No.2, pp. 270-293, 1997.
[22] S. Ubukata, S. Sekiya, A. Notsu, and K. Honda, "Noise Rejection Scheme for Rough Set-Based C-Means Clustering," Proc. of 16th Int. Conf. on Modeling Decisions for Artificial Intelligence, pp. 70-81, 2019.
[23] Q. Hu, D. Yu, and Z. Xie, "Neighborhood classifiers," Expert Systems with Applications, Vol.34, Issue 2, pp. 866-876, 2008.
[24] Q. Hu, D. Yu, J. Liu, and C. Wu, "Neighborhood rough set based heterogeneous feature subset selection," Information Sciences, Vol.178, Issue 18, pp. 3577-3594, 2008.
[25] Y. Y. Yao, "Generalized Rough Set Models," L. Polkowski and A. Skowron (Eds.), "Rough Sets in Knowledge Discovery 1: Methodology and Applications," pp. 286-318, Physica-Verlag, 1998.
[26] UCI Machine Learning Repository, http://archive.ics.uci.edu/ml/ [accessed March 20, 2020]

Name:
Seiki Ubukata

Affiliation:
Graduate School of Engineering, Osaka Prefecture University (OPU)

Address:
1-1 Gakuen-cho, Nakaku, Sakai, Osaka 599-8531, Japan

Brief Biographical History:
2014- Assistant Professor, Graduate School of Engineering Science, Osaka University
2015- Assistant Professor, Graduate School of Engineering, OPU
2020- Associate Professor, Graduate School of Engineering, OPU

Main Works:
• "Characteristics of Rough Set *C*-Means Clustering," J. Adv. Comput. Intell. Intell. Inform., Vol.22, No.4, pp. 551-564, 2018.
• "A Unified Approach for Cluster-Wise and General Noise Rejection Approaches for K-Means Clustering," PeerJ Computer Science, 5:e238, doi: 10.7717/peerj-cs.238, 2019.

Membership in Academic Societies:
• The Institute of Electrical and Electronics Engineers (IEEE)
• Japan Society for Fuzzy Theory and Intelligent Informatics (SOFT)
• The Institute of Systems, Control and Information Engineers (ISCIE)
• Japan Society of Kansei Engineering (JSKE)

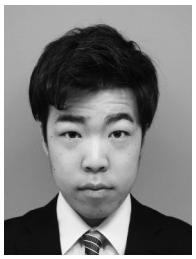

Name:
Sho Sekiya

Affiliation:
Graduate School of Engineering, Osaka Prefecture University (OPU)

Address:
1-1 Gakuen-cho, Nakaku, Sakai, Osaka 599-8531, Japan

Brief Biographical History:
2019 Received the B.Eng. degree in Department of Computer Sciences and Intelligent System, OPU

Main Works:
• "Noise Rejection Scheme for Rough Set-Based C-Means Clustering," Proc. of 16th Int. Conf. on Modeling Decisions for Artificial Intelligence, pp. 70-81, 2019.

Name:
Akira Notsu

Affiliation:
Graduate School of Humanities and Sustainable System Sciences, Osaka Prefecture University (OPU)

Address:
1-1 Gakuen-cho, Nakaku, Sakai, Osaka 599-8531, Japan

Brief Biographical History:
2005- Research Associate, Graduate School of Engineering, OPU
2007- Assistant Professor, Graduate School of Engineering, OPU
2012- Associate Professor, Graduate School of Engineering, OPU
2016- Associate Professor, Graduate School of Humanities and Sustainable System Sciences, OPU
2020- Professor, Graduate School of Humanities and Sustainable System Sciences, OPU

Main Works:
• "Visualization of balancing systems based on naïve psychological approaches," AI & Society, Vol.23, No.2, pp. 281-296, 2009.
• "Visualization of Learning Process in "State and Action" Space Using Self-Organizing Maps," J. Adv. Comput. Intell. Intell. Inform., Vol.20, No.6, pp. 983-991, 2016.

Membership in Academic Societies:
• The Society of Instrument and Control Engineers (SICE)
• Human Interface Society (HIS)

Name:
Katsuhiro Honda

Affiliation:
Graduate School of Engineering, Osaka Prefecture University (OPU)

Address:
1-1 Gakuen-cho, Nakaku, Sakai, Osaka 599-8531, Japan

Brief Biographical History:
1999- Research Associate, Graduate School of Engineering, OPU
2007- Assistant Professor, Graduate School of Engineering, OPU
2009- Associate Professor, Graduate School of Engineering, OPU
2013- Professor, Graduate School of Engineering, OPU

Main Works:
• "Linear Fuzzy Clustering with Selection of Variables Using Graded Possibilistic Approach," IEEE Trans. on Fuzzy Systems, Vol.15, No.5, pp. 878-889, 2007.
• "Fuzzy PCA-Guided Robust *k*-Means Clustering," IEEE Trans. on Fuzzy Systems, Vol.18, No.1, pp. 67-79, 2010.

Membership in Academic Societies:
• The Institute of Electrical and Electronics Engineers (IEEE)
• Japan Society for Fuzzy Theory and Intelligent Informatics (SOFT)
• The Institute of Systems, Control and Information Engineers (ISCIE)
• Japan Industrial Management Association (JIMA)